Photodegradation of typical Mediterranean plant litters: variations with Quercus species and the leaf-surface exposed

Anne Marie Farnet da Silva, Lisa Foli, Jean-Luc Boudenne, Fabio Ziarelli, C Rebufa

Photodegradation of typical Mediterranean plant litters: variations with *Quercus* species and the leaf-surface exposed

Anne-Marie Farnet Da Silva[1],·Lisa Foli[1],·Jean-Luc Boudenne[2],·Fabio Ziarelli[3],·Catherine Rebufa[1]

[1] Aix Marseille Univ, CNRS, IRD, Avignon Université, UMR IMBE 7263, Marseille, France

[2] Aix Marseille Univ, CNRS, LCE, Marseille, France

[3] Spectropole, Fédération Des Sciences Chimiques de Marseille, Aix Marseille Univ, CNRS, Campus St Jérôme,13397 Marseille, France

Abstract

Photodegradation can play a key role in litter decomposition under the context of climate change which hinders organic matter turnover because of available water scarcity. Here, we aimed at testing the effect of a two-month sunlight exposure with different radiation intensities (either in winter or summer) on the chemical signature of two typical Mediterranean species, i.e., *Quercus ilex* and *Q. pubescens*. We also tested whether the side of the leaf exposed mattered in the chemical modification observed. To do so, two holistic chemical approaches, FTIR-ATR (Fourier transform infrared–attenuated total reflectance) and solid-state NMR of 13C, were used. ANOVA from solid-state NMR of 13C revealed that after exposure in summer, certain markers of lignin (phenol and aromatics) decreased in leaves whatever the Quercus spp. and it depended on the side of the leaf exposed. Lignin transformation thus occurred via dearomatization and/or dephenolization. Moreover, for both species, when leaves were exposed at their topside, their NMR chemical signatures were negatively correlated with alkyl assigned to cutin and waxes, showing that the thin layer of cuticle was attacked by photodegradation. FTIR-ATR spectra and NMR data also highlighted that a weaker irradiation (winter vs summer exposure) strongly limited lignin content decrease. Finally, lignin, cutin and wax oxidation, by enhancing the availability of polysaccharides from lignocellulose, may favor further litter transformation when suitable climate conditions (mainly humidity) are recovered.

1. Introduction

Plant litter decomposition is key in ecosystem functioning since organic matter decomposition sustains C and N turnover, primary production and also C sequestration in soils. This process is driven by various factors and their interactions, i.e., microbial communities, the quality and quantity of litter, climate conditions (mainly temperature and humidity) at various geographical scales (Boukhdoud et al. 2016, Coûteaux et al., 1995, Kheir et al. 2020a and b). Climate change can impact mineralization directly, by affecting microbial communities and their activities, and indirectly, by inducing plant responses to such stresses and thus modification in plant chemistry (Suseela and Tharayil, 2018). Many efforts have been recently devoted to establishing the effects of climate change on plant chemical properties, i.e., elemental compositions of leaves and root (Sardans et al., 2017) or modifications of chemical components such as cutin and waxes with higher proportions of longer aliphatic compounds (Heredia-Guerrero et al., 2018). In Medi-terranean forests, higher temperatures and more drastic and prolonged periods of drought induce an increase in the recalcitrant fraction of plant material, i.e., mainly phenols and terpens (Suseela and Tharayil, 2018) which is supposed to limit litter biodegradability.

Under this context, photodegradation may play a crucial role by mitigating the drastic effects of summer drought on microbial activity performance in litter decomposition and by enhancing litter decomposition when more favorable climate conditions are recovered (autumn). Photodegradation can indeed control litter mass loss directly, by breaking down molecules and releasing CO_2, and indirectly, by favoring substrate availability for microbial activities (Duguayand and Klironomos, 2000). Microbial facilitation via photodegradation ("photopriming") has been proved in litters from arid and semiarid ecosystems (Day et al. 2007, 2015) by converting large polymers such as lignin to smaller and easily degradable molecules and reducing the bottleneck imposed by lignin in secondary cell walls. Also, in deserts, a dependence of the effects of UV photodegradation of litter (shrubs, summer, and spring annuals) decomposition on rainfall has been observed: Photodegradation effects were not strongest in the driest region (Huang et al., 2017) and litters decomposed faster under high-frequency than low-frequency precipitations (Huang and Li 2017). However, no rainfall effects were significant on the UV degradation of leaf litter composed with a native shrub and an exotic annual grass (Esch et al. 2019). Lignin is the main target of photodegradation because of its spectroscopic properties. UV-B (280-320 nm) and UV-A (320-400 nm) are the major radiations of the light spectrum involved in photodegradation (Austin and Vivanco2006; Brandt et al. 2007). Previous studies have underlined the importance of the type of litter on the efficiency of photodegradation (Day et al. 2018; Kirschbaum et al., 2011; Hunt and Seveny, 2002) since the quantity of molecules absorbing UV varies with this factor. The effects of UV photodegradation are greater in litter with low lignin content than in litter with high initial lignin content. Spring annuals, with high relative growth rates, would rarely develop protective/defensive structures and would therefore be more sensitive to UV radiation. In addition, the surface of the leaves and the proportion of lignin should also be factors to consider when studying the effects of UV photodegradation (Huang and Li, 2017). Herbaceous and shrub litter were proved to be more sensitive to photodegradation than tree litter, showing a greater mass loss after irradiation (Wang et al. 2020).However, contrasted results have been revealed concerning the effect of UV exposure on litter chemical modification: Litter loss weight was reported after UV radiation exposure under laboratory experiment depending on the plant species, the wavelength and the exposure time used (Brandt et al., 2007; Day et al., 2007; Pieristé et al., 2020a, b), while Lambie et al. (2014) did not find any modification of litter composition after photodegradation. Thus, more information is still needed to shed light on the impact of photoradiation on Mediterranean litters under the context of climate change. Here, we explore how exposure to sunlight in the field modifies the chemical composition of two typical Mediterranean tree species *Quercus ilex* and Quercus *pubescens*. In the case of *Q. pubescens*, photodegradation may play an important role because of its marcescent foliage, this specific ecophysiological trait leading to longer and direct exposure time in autumn and winter. We indeed focused on the irradiation effect that may occur in the field: leaves freshly fallen were exposed two months during either winter or summer to test the effect of various intensities of radiations without considering further microbial decomposition step. Moreover, for these Mediterranean leafy species, we also tested the effect of the side of the leaf exposed since both species exhibit different chemical composition depending on the surface: a wax-rich cuticleon the topside compared to the back side. We proposed a different approach of that commonly used (based on mass loss of litter, specific leaf decomposition rate, C/N ratio, lignin content...) by following the variations of the leaf chemical composition after light exposure, from their spectral signatures, obtained by two chemical nondestructive holistic approaches, i.e., infrared spectroscopy and solid-state NMR of 13C. Both techniques have been proved to be useful tools to describe organic matter "fingerprint" in litters and soils and discriminate chemical signature depending on plant species and decomposition stage (Farnet-Da Silva et al., 2017; Delcourt et al., 2019; Richardson et al., 2004). The individual response of *Quercus ilex* and *Quercus pubescens* litters is considered an important preliminary step toward a better

understanding of multi-species litter decomposition (site of synergistic and antagonistic interactions), irrespective of the role of heterotrophic soil decomposer microorganisms.

2. Material and methods

2.1. Site description and litter sampling

Leaves of *Quercus ilex* and *Q. pubescens* from the top layer of litter were collected in June 2018 near Aix en Provence in the Massif de la Trévaresse (43°38'31.54''N; 5°26'1.11''E) in three independent sites (« Château Féline», « le Coucou»and « la Quille») with similar pedologic and topographic characteristics: around 200 m in elevation, northeastern exposure, slope (10 to 15%) and soil type (Calcaric Leptosol according to IUSS Working Group WRB, 2006). Fourteen leaves were collected from each site for a total of 6 samples (3 sites × 2 species).

2.2. Sunlight exposure

Conversely to some studies assessing how UV radiation, the seasonal canopy phenology, the litter layer thickness or their interaction may affect litter photodegradation (Wang et al., 2020; Mao et al., 2018), the scenario chosen here was to expose leaf litter under the full spectrum of sunlight at two different seasonal periods and by differentiating the exposed leaf face. Each leaf was cut in two pieces, and then, each part was pinned on a polystyrene board with either the top or the back side (later called top and bottom, respectively) exposed to sunlight (Fig. 1). 12 half leaves (7 per exposed side, above and below) for each specie were used in triplicate (3 sites). Thus, 7 half leaves for each species and for each side were exposed for two months in summer (July and August 2018) and winter (late December–mid-February 2018–19) fora total of 168 samples (2 seasons × 3 sites × 2 species × 7leaves × 2 sides).

Fig. 1: *Quercus ilex* and *Quercus pubescens* sampling:12 half leaves (top and bottom side alternatively) for each species

One sampling was performed after the two-month exposure in either winter or summer. The experiments were set up in the botanical garden of the Faculty of St Jérôme (Marseille, France). Radiation measurement (measure of irradiance in W/m2) was taken at noon once a week during all the experiment using Radiometer HD 90–20(Oriel, Newport). The dynamic range of the instrument in

the various scales goes from 100 nanowatt/cm^2 to 200 milliwatt/cm^2. Different radiometric probes were used: an HD9021 UV-B in the UV-B wavelength of 280–315 nm, an HD9021 UV-A in the UV-B wavelength of 315–400 nm and an HD 9021 RAD/C in the visible wavelength of 400–900 nm. The average of measured values for UV-A, UV-B and visible irradiance was of 11.3, 4.4 and 726.5 W/m^2 in summer and 2.8, 1.2 and 311 W/m winter. A compilation of irradiance solar data in Marseille showed that the average annual value of global irradiance is between 189 and 219 (kWh/m^2 cumulated) for July and August months and decreases to 46–67 from December to February (CalSol software, INES). After exposure, the 168 samples were analyzed according to the exposed face with FTIR-ATR technique. For 13C NMR analyses, litter samples were analyzed as composite samples of7 half leaves: 24 composite samples (2 seasons × 3 sites × 2species × 2 sides) were reduced to powder using a steel bullet blender Retsch MM40 (Fisher Scientific, France).

2.3. Chemical characterization of litters by FTIR-ATR (Fourier Transformed Infrared–Attenuated Total Reflectance) and by solid-state NMR of 13C

The exposed face (top or bottom) of the entire leaf of either *Q. ilex* or *Q. pubescens* was directly deposited, onto a Specac's Golden Gate™ ATR Accessory of a ThermoNicolet IS10 spectrometer equipped with a Mercury Cadmium Telluride (MCT) detector, an Ever-Glo source and a KBr/Ge beam splitter. Spectra were acquired between 4000and 650 cm−1, with a 4 cm−1 nominal resolution. For each spectrum, 100 scans were co-added. A background spectrum in air (under the same acquisition conditions as those used for the samples) was acquired before each acquisition. The ATR crystal was carefully cleaned with ethanol to remove any residual traces of the previous sample. Ten spectra were recorded for each sample in order to examine the whole exposed face. OMNIC 8.1 (Thermo Nicolet) was used to record FTIR-ATR spectra. The Unscrambler version10.3 from computer-aided modeling software (CAMO, Trondheim, Norway) was used to perform data analyses.

The spectral range of the absorption of the carbon dioxide was removed (between 2400 and 1900 cm−1), and then, two preprocessing methods were applied: a multiplicative scatter correction (MSC) to remove from the spectra the slope variation caused by scatter and variation in particle size. CP/MAS 13C NMR spectra of litter powder were obtained on a Bruker DSX 400 MHz spectrometer operating at100.7 MHz. Samples (600 mg) were spun at 10 kHz at the magic angle. Contact times of 2 ms were applied with a pulse width of 2.8 µs and a recycle delay of 3 s. Chemical shift values were referenced to glycine signal (carbonyl Cat 176.03 ppm). Chemical shift values were referenced to glycine signal (carbonyl C at 176.03 ppm). Seven common chemical shift regions were defined according to Mathers et al. (2007): alkyl C (0–45 ppm), methoxyl C (45–60 ppm), O-alkyl C (60–92 ppm), di-O-alkyl C (92–112 ppm), aromatic C (112–142 ppm), phenolic C (142–160 ppm)and carboxyl C (160–185 ppm). Dmfit 2003 software was used to determine the intensity of each chemical shift region (Massiot et al., 2002). An aromaticity ratio was also calculated to estimate the proportion of aromatic compound sin each litter (Baldock et al., 1997).

2.4. Statistical analyses

For NMR data, the normality and homogeneity of the variances of the data were determined on the residuals from the regression model with the Shapiro–Wilk and Levene tests, respectively. Data were transformed to common logarithms, log10, when necessary to meet the requirements of normality and homogeneity of variance for ANOVA. Three-way ANOVA was used to determine whether, and to what extent, NMR data depended upon i) litter type, ii) the side of the leaf exposed, iii) the season of exposure and iv) their interactions. When a three-way interaction was found, we separated data for each modality of treatment and type of litter and environmental context using a one-way ANOVA. Statistically significant ($P < 0.05$) main effects and interactions were further analyzed using the Tuckey

HSD post hoc tests. NMR data were also analyzed via principal component analyses (PCA) using the NMR peaks from each sample of either *Q. ilex* or *Q. pubescens* after a two-month exposure to describe chemical changes of the leaf composition depending on the factors tested (winter vs summer, top or back side of the leaf, *Quercus spp*). PCA was also used to detect variations in the FTIR spectral dataset in correlation with chemical characteristics of the litters, the season and the side of the leaf exposed. Principal components (PC)were extracted with a full cross-validation on centered and reduced data. PCA was used to facilitate the analysis of spectral information by grouping data into smaller sets and eliminating multi-collinearity between variables (wave number). This approach enabled us to explain the variance observed in the initial data set, by extracting a reduced number of principal components (PCs) defined as pure and simple mathematical transformations of the initial variables. PCA results were interpreted through the graphical representation of the sample in the factorial plane of the principal components (score plot) and those of the variables in the same factorial plane (loading plot). The sample grouping in the factorial plane was interpreted through their position (positive or negative) on one of the axes. In parallel, the examination of the PC loadings showed which spectral bands were predominant in the sample grouping, in either the positive or negative part of the PCs (Jolliffe 2002).

3. Results

3.1. Solid-state NMR of 13C characterization of leaves after photodegradation

The three-way ANOVA revealed an effect of the season of exposure: variations in the NMR signals were observed after exposure in summer only. We thus further considered data obtained from this season of exposure. The two-way ANOVA showed significant effects of the interaction between Quercus species and the side of the leaf exposed on both phenolic ($F = 7.542$, $p < 0.005$) and aromatic ($F = 9.365$, $p < 0.001$) signals (Fig. 2a and b). Phenolic amounts decreased to a similar extent whatever the side of the leaf exposed for Quercus pubescens, while for Quercus ilex, a higher decrease in phenols was observed when the side below was exposed (Fig. 2a). For aromatic compounds, we found no differences between control and exposed leaves for *Quercus pubescens*, while for *Quercus ilex*, a strong decrease in aromatics was found whatever the side of the leaf exposed (Fig. 2b).

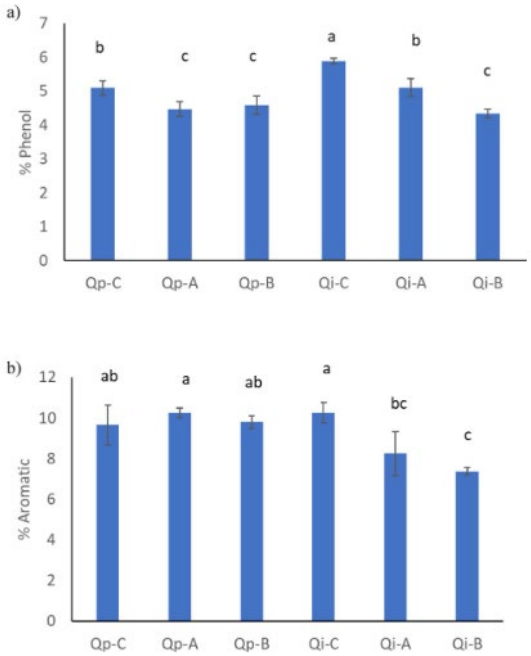

Fig. 2: NMR signals of phenol % (a) and aromatic % (b) from *Quercus ilex* (Qi) and *Quercus pubescens*

PCA were performed on NMR data for both Quercus species and for the two seasons of irradiation. Results are shown in Figs. 3 and 4 (summer and winter exposure, respectively), and each projection represents the barycenter of three samples (14 leaves per sample).

After a 2-month exposure in summer (Fig. 3), differences between projections were observed depending on the Quercus species considered and on the side of the leaf exposed. For Q. ilex leaves (Fig. 3a), PCA revealed that the side of the leaf exposed led to differences in chemical com-position according to PC1 (61.7% of variance) and that control was discriminated from photoxidized leaves according toPC2 (23.7% of variance). Topside-exposed leaf (Qi-A) was discriminated from bottom-side exposed leaf (Qi-B) according to PC1, showing a different impact of photodegradation depending on the surface exposed, probably because of the thin layer of cuticle particularly rich in cutin and waxes.

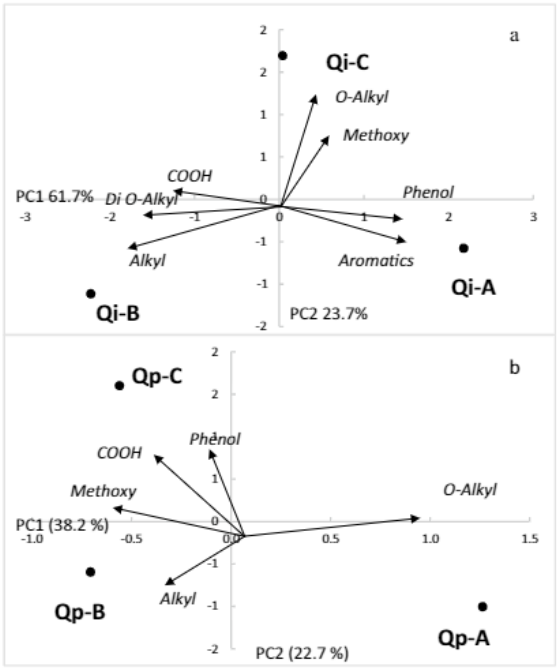

Fig. 3: PCA of (a) *Quercus ilex* (Qi) and (b) *Quercus pubescens* (Qp)leaves which surface were exposed to sunlight radiations at the top (a) or bottom (b) side or not exposed (c) during two months in summer (July and August 2018).

Control projection was explained by O-alkyl and methoxy, while projections of top- and bottom-side-exposed leaf (Qi-A and Qi-B) were explained by phenol and aromatics on the one hand and alkyl on the other hand. It has to be noted that Qi-A was negatively correlated with alkyl signal usually assigned to cutin and waxes.

For *Q. pubescens* (Fig. 3b), PCA clearly revealed a similar trend as that observed for Q. ilex: a discrimination between projections linked to the two types of surfaces exposed was observed according to PC1 (38.2% of variance), while control and exposed leaved (whatever the exposed side) were separated according to PC2 (22.7%). However, and conversely to what was found for Q. ilex leaves, NMR signal assigned to lignin (i.e., phenol) was associated with control Qp-C, indicating that lignin transformation, via dephenolization, may occur during photodegradation o fboth sides of the leaves. More precisely, phenol and COOH explained the projection of control, while alkyl and O-alkyl explained the projections of Qp-B and Qp-A, respectively. For *Q. pubescens* too, alkyl, linked to cutin and waxes, was thus negatively correlated with the chemical signature of the topside-exposed leaves essentially characterized by the O-alkyl fraction (polysaccharides).

After a 2-month exposure in winter, different tendencies from those observed after summer exposure were found for Q. ilex and Q. pubescens. For both Q. ilex and Q.pubescens (Fig. 4a and b), controls were differentiated from exposed leaves according to PC1 (48% and 47.5% of variance, respectively). For *Q. ilex*, control projection was explained mainly by aromatics and phenols, while exposed leaves were positively correlated with a signal assigned to polysaccharides, i.e., O-alkyl. For *Q. pubescens*, control was explained by methoxy, and O-alkyl and exposed leaves were also mainly associated with a signal assigned to polysaccharides, i.e., di-O-alkyl.

3.2. Infrared characterization of leaves after photodegradation

Average and MSC corrected FTIR-ATR profiles (Fig. 5) of *Q. ilex* and *Q. pubescens* leaves were different according to the topside- or bottom side exposed (or not) to sunlight radiations and according to the season (summer or winter). Spectral modifications were visible on characteristic bands of polysaccharides (cellulose, hemicellulose and pectins), waxes (mixtures of alkanes, alcohols, aldehydes, fatty acids and esters) and lignin (a complex heteropolymer based on phenylpropanoid subunits with methoxy groups). The 3000-2700 and 720-700 cm^{-1} regions (Table 1) assigned to aliphatic material (symmetric and asymmetric CH2 andCH3 stretching and CH bending vibrations, respectively)showed bands with different intensity according to the wax composition of the leaf side, which varied according to litter species and the seasonality exposure. For instance, topside of *Q. ilex* leaves was richer in waxes than the bottom side. Numerous spectral bands between 1500 and 1100 cm^{-1} and between 900 and 750 cm^{-1} (Table 1) associated with carbohydrates (CN of amides, C-O of ester, alcohol and pyranose ring) or phenylpropanoid rings showed variations after photodegradation, indicating conformation modifications of litter cell wall.

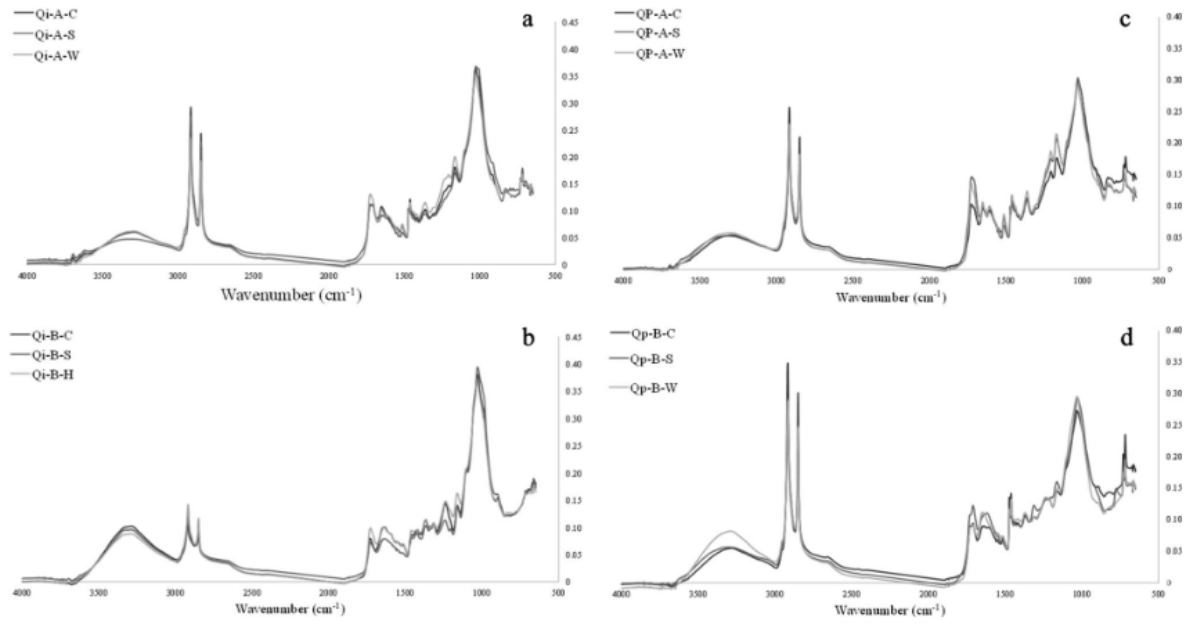

Fig. 5: FTIR-ATR average and MSC corrected profiles of *Quercus ilex* (a, b) and *Quercus pubescens* (c, d) leaves with the top- (a) or bottom-(b) side surfaces exposed to sunlight radiations or not exposed (c) during summer (S) and winter (W) month.

In order to extract the information due to the variance of spectral modifications, PCAs were performed on infrared spectroscopic data from leaves exposed in summer and in winter and for each species.

For *Q. ilex* and when the topside of the leaf was exposed (Fig. 6a), projections from summer exposure were clearly separated from those from winter exposure according to PC1(52% of variance). After

winter exposure, projections were explained by signals at 2929, 2858 and 721 cm^{-1}, characteristic of the asymmetrical and symmetrical stretching vibration of CH2 groups and of a C-H rocking vibration at 1724,1228 and 1169, cm^{-1} from C = O stretching of ester functional groups, C–O from alcohols and a C–O–C asymmetrical stretching vibration band from esters (Fig. 6b, Table 1).

These signals are thus characteristic of long aliphatic chains mainly found in cutin and waxes. Projections after winter exposure were also characterized by signals from aromatic skeletal, i.e., signals at 1516 and 1440 cm^{-1} from C = C stretching of aromatic rings and from phenols, at 1359 $cm^{-1}$and 1228 cm^{-1} from O–H deformation and C–O stretching of phenolics (Table 1). On the other hand, after summer exposure, leaves were characterized by polysaccharides, i.e., C–O–C signal (ring stretching) from glycosides (1005 cm^{-1}) and pyranose ring (914 cm^{-1}) (Table 1).

Table 1: Main functional groups assigned to the different vibrations present in FTIR-ATR spectra and PCA loading of *Quercus ilex* and *Quercus pubescens* leaves which surfaces were exposed to sunlight radiations at the top (Top) or back (Bottom) side during two months in summer or winter

Assignations	Wave number (cm^{-1})							
	Quercus ilex				*Quercus pubescens*			
	Top		Bottom		Top		Bottom	
	Summer	Winter	Summer	Winter	Summer	Winter	Summer	Winter
O–H stretch, H-bonded	3610	3286		3310		3293		3296
C–H stretch methyl and methylene groups		2929	2916	2937		2916		2914
C–H stretch O–CH_3 group		2858	2850			2848		2848
C=O stretch, unconjugated ketone, carboxyl and ester groups	1724		1699	1734	1745, 1710		1735	
Amide I band (C=O stretch, C–N or N–H in-plane deformation)		1652		1643		1649		1657
Ring-conjugated C=C				1643		1649		
Ring C–C stretch of phenyl (symmetric)							1610	
Amide II band or Ring-conjugated C=C				1541				
Ring C–C stretch of phenyl (asymmetric)		1516				1518		1518
CH_2 bending of the methylene chains			1473					
CH_2 scissoring mode of the acyl chains						1464		1462
CH_2 bending mode		1440						
O–CH_3, C–H or N–H deformation symmetric		1359		1373		1361		
Amide III band, CH_2 stretch							1315	
C–O stretch, Amide III band								1252
C–C, C–O and C=O stretches		1228		1230				
CO–O–C, C–O, C–OH stretches		1169					1172	
C–O, C–C ring stretches				1124				
C–O deformation				1076				1078
C–O, C–C ring stretches, C–OH bonds of polysaccharides, –CH=CH out-of-plane bending	1005, 914	1000, 912			1005, 927	989, 941		
C–H wagging in methylene group		883						
Guanine C3-endo/syn conformation	796				794			
C=C–H deformation of aromatic ring							777	
C–H in-plane rocking in methylene group								730
C–H in-plane rocking in methylene group		721	719			719		717

When the bottom side of the leaf of Q. ilex was exposed (Fig. 6c), projections were discriminated depending on the season according to PC2 (19% of variance). After winter exposure, projections were explained by similar signals compared to leaves exposed at the topside: 1734 cm^{-1} from conjugated carbonyl (C = O) stretching of ester functional groups, 1541 cm^{-1} from C = C of aromatics and signals from alcohols, i.e., 1373, 1230, 1076 cm^{-1} (Fig. 6d). After summer exposure, leaf chemical signature was characterized by polysaccharides, i.e., C–O–C signal from glycosides(1000 cm^{-1}) and pyranose ring

(912 cm^{-1}) as described top and conversely to leaves exposed at the topside, by signals from alkyl chains from cutin and waxes at 2916, 2850 and 719 cm^{-1}, characteristic of the asymmetrical and symmetrical stretching vibration of CH2 groups and of a C–H rocking vibration of long chains (Fig. 6d).For *Q. pubescens*, when the topside of the leaf was exposed, quite similar results as those found for *Q. ilex* were observed. Discrimination between summer and winter exposures was observed according to PC2 (27% of variance) (Fig. 7a and c). The chemical signature of topside-exposed leaves after winter exposure was explained by signals from long alkyl chains (2916, 2848 and 719 cm^{-1}) and from aromatic skeletal and phenols (i.e., 1518 and 1464 $cm^{-1}$from C = C of aromatic rings and phenols, O–H deformation of phenolics at 1361 cm^{-1}) (Fig. 7b). After summer exposure, signals linked to C = O from aliphatic ester and acid (1745 and 1710 cm^{-1}) and those linked to polysaccharides C–O–C signal from glycosides (1005 cm^{-1}) and pyranose ring (927 cm^{-1}) explained leaf chemical signature. When the bottom side was exposed, discrimination between winter and summer exposure was observed according to PC2 (24% of variance) (Fig. 7c). Under these conditions, similar results as described top were found after winter exposure: leaf chemical signature was mainly explained by signals from long alkyl chains (2914, 2848 and 728 and 717 cm^{-1}) with hydroxyl groups (C–O stretching at 1078 cm^{-1}) and conjugated C = O (1657, 1462 cm^{-1}) (Fig. 7d). After summer exposure, bottom-side-exposed leaf projections were explained by signals of C = O of aliphatic esters (1736 cm^{-1}), of aromatics (C = C skeletal stretching vibrations at 1610 cm^{-1} and = C–H out-of-plane bending at777 cm^{-1}) and pyranose ring at 989 and 941 cm^{-1}.

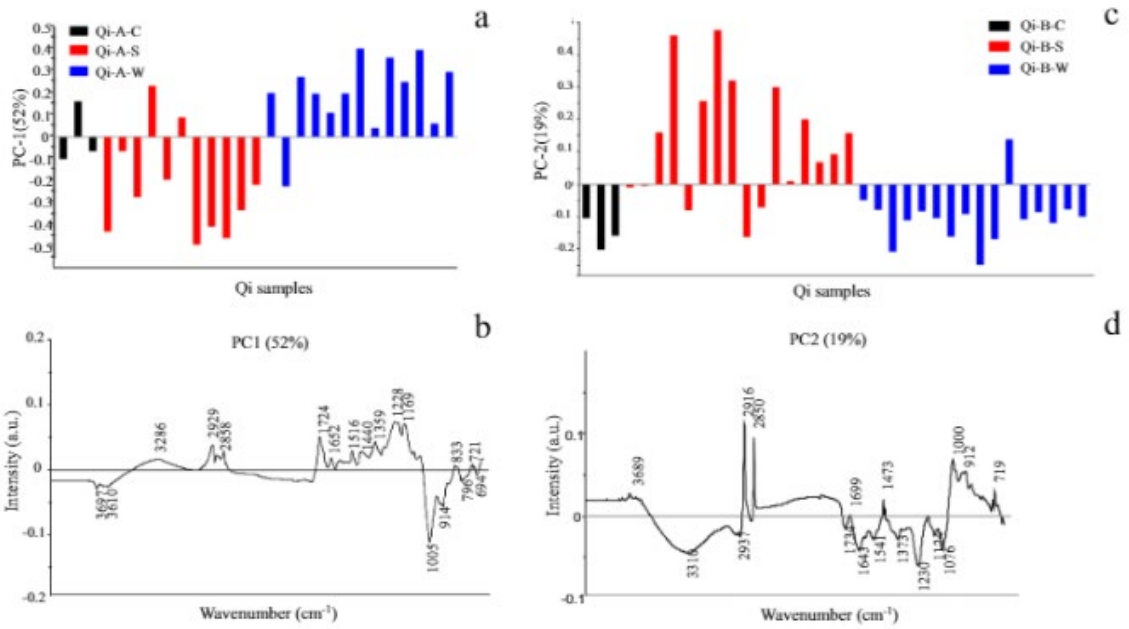

Fig. 6: PCA of FTIR profiles of *Quercus ilex* (Qi) leaves with the top (a) and bottom (b) surfaces exposed to sunlight radiations or not exposed(c) during summer (S) and winter (W) months. PC1 and PC2 scores (a and c) and loading (b and d) plots

4. Discussion

Photodegradation can play a major role in the predegradation of litter debris under the context of climate change leading to limited resources in water, which hinders biological transformation and organic matter turnover (Huang et al., 2017).

In our study, NMR and FTIR-ATR were used as holistic chemical approaches to characterize leaf chemical modifications after a two-month exposure either in summer or winter. Photodegradation of

the chemical leaf structure was actually found after exposure in summer, which can be explained by the huge difference in intensity of radiation between winter and summer, especially under the Mediterranean con-text. NMR results from PCA revealed that for both species, controls were associated with markers of lignin (phenols and also methoxy functions found in certain aromatic monomers of lignin, i.e., coniferyl and sinapyl alcohols), while exposed leaves were negatively correlated with these markers indicating that lignin was less abundant in their chemical structure after sunlight exposure. These results were confirmed by the ANOVA, showing a significant decrease in lignin markers (both phenol and aromatic) after the two-month exposure in summer. This goes in line with previous studies which showed a decrease in lignin chemical markers after photodegradation. Lin et al. (2015) found that UV exposure reduced the major lignin structural units including aryl ether linkages (guaiacyl linkages) and the relative abundance of p-hydroxyphenols. Almagro et al. (2015) demonstrated that UV exposure of leaf litters from *Stipa tenacissima* induced lignin loss and favored overall litter transformation yields by enhancing the release of soluble compounds from plant cells. This latter result was also shown by Gallo et al. (2006) for *Pinus edulis* and *Juniperus monosperma* litters, indicating that photodegradation can have a direct effect on lignocellulose structure and an indirect effect on litter decomposition by increasing the amount of dissolved organic compound availability. Results from Austin et al. (2016) showed that solar radiations have reduced lignin concentrations of different litter species from temperate ecosystems of South America and that blue and green wavelengths (400–550 nm)have a greater effect than UV light because of the strong light absorbance of lignin in this spectral region and the high relative proportion of blue and green radiations with respect to UV quanta in solar spectrum. Wang et al. (2020) confirmed that lignin was subject to photochemical mineralization after a sunlight exposure and particularly, under blue light because of its strong absorbance in this spectral region compared to UV-B zone. They quantified that blue light has contributed 75% of litter decomposition rates after a litter exposure to the full spectrum of sunlight. In parallel, these authors also showed that polyphenolic compounds played an important role because leaf litter with higher poly-phenolic content promoted UV-B photodegradation in the understorey. Together with an increase in cellulose avail-ability and biodegradability, “photopriming” may thus play an important role in organic matter decomposition under the context of water scarcity due to climate change (Bornman et al., 2014; Foereid et al., 2010; Wang et al., 2015).

However, the decrease in phenols varied with the side of the leaf exposed for Quercus ilex, with a weaker decrease when the top of the leaf was exposed. This result can be linked to the thick layer of cutin and waxes (Farnet Da Silva et al., 2017) that is particularly observable for this Quercus species. Moreover, PCA shows that when leaves were exposed at their topside, their NMR chemical signatures were negatively correlated with alkyl compounds and this result was obtained for both Quercus species. This type of molecules is known to be assigned to long fatty acid and alcohol chains found in cutin and waxes. This shows that, after sunlight exposure at the topside, the typical signal of cuticle is less preponderant in the chemical signature of Quercus spp. leaves probably because of photodegradation. The study of Feng et al. (2011) indeed revealed that aliphatic signals from solid-state NMR of 13C data of *Pinus taedaneedles* decreased after photodegradation under laboratory conditions using UV-B irradiance comparable to summer in the midlatitude for 1 to 3 months. This result is corroborated by the study of Day et al. (2007) who subjected litters of *Larrea tridentata* to different solar UV-B exposures in the Sono-rian desert (Arizona) and found that concentrations in lipids declined, underlining the importance of UV-B-driven photodegradation. The fact that cuticle can be efficiently photooxidized is of particular importance for *Q. pubescens* as a marcescent species. A preoxidation of the chemical structure of the leaves, while it remains in the canopy in autumn and later in winter, will thus probably occur prior to active biological decomposition after falling onto litter (Table 1).

When considering FTIR data, our results revealed that the intensity of the radiation, assessed via either summer or winter exposures, strongly influenced the chemical signature of leaves. Moreover, few differences were observed according to the leaf surface exposed or the Quercus species. Gallo et al. (2006) explained that lignin reduction was species-dependent (in their study, *Pinus edulis* vs *Juniperus monosperma*) and that this was prob-ably due to species-specific litter chemistry, mainly phenol concentrations and linkages between phenylpropane units in the plant structure. The relative proportions ofβ-Aryl ether (β-O-4), α -Aryl ether (α-O-4) and diphenylether (4-O-5) linkages indeed differ between plant species (softwood and hardwood lignins, grass lignin), explaining the intensity of photodegradation effects. Lanzalunga and Bietti (2000) described the reactivity of lignin to photo-degradation using models including different lignin structural motifs. Here, similar lignin structures in *Quercus spp*. as hardwood lignin species, probably explained the homogeneity of the results found. FTIR analyses showed that aromatics, phenols and alkyl signal assigned to lignin or cutin and waxes, respectively, were clearly less intense after summer exposure. Day et al. (2015), in a study com-paring the effect of sunlight vs irradiance without UV or without UV-B on litter photodegradation of Cynodon dactylon and *Larrea spp*., underlined the important contribution of UV in litter transformation, though their impact were not proportional to lignin content. Consequently, in our study, less intense UV radiations during winter have probably led to a weaker impact on the chemical signature of leaves, whatever the side exposed.

In this study, modifications in the chemical signature of leaves were found after a 2 month exposure. It has to be noted that many studies on litter photodegradation used litter bags to expose plant debris to natural sunlight (Huang et al., 2017). This methodology thus may include overlapping of plant materials, which reduced the leaf surface exposed. Here, each leaf was pinned on a board to maximize the surface irradiated, which probably explains the photodegradation effect on leaf chemical signature after a 2-month exposure. Moreover, it has to be noted that photodegradation in natura strongly depends on the intensity of UV radiations depending on biomes, on the covering canopy phenology (in deciduous forests), on the relative proportion of gaps vs understorey in the forests and thus on tree density (Wang et al., 2022). In tropical forests, where the cover of the canopy is intense, UV radiation alters the chemistry of lignin and cellulose increasing their degradability and facilitating microbial degradation ("photo-facilitation") (Jiang et al., 2021). In more arid climates, the direct light-induced degradation during the drought season can strongly be involved in litter mineralization. Under the context of climate change, the effects of this process should be considered as an important driver of organic matter turnover in dryland ecosystems (Gliksman et al., 2017).

5. Conclusion

Photodegradation of plant debris can play a major role in plant decomposition by counteracting the effect of climate change in arid and semiarid regions. Our study revealed that lignin contents in leaves from two typical Mediterranean species particularly rich in cutin, can be efficiently lowered after sunlight exposure and this is noticeably interesting for marcescent species such as *Quercus pubescens*, whose leaves are longer exposed to UV. Further studies should include the biological component of litter to shed light on the effect of such prephotodegradation on the kinetics of decomposition process.

Acknowledgements

We would like to thank our Research Unit, the Mediterranean Institute of Biodiversity and Ecology, for the funding of this work via its intern call for proposals. Many thanks to Dr. ArneSaatkamp to facilitate the access to the Botanical Garden of St Jerome which is part of the common service "Experimental Devices" of the Mediterranean Institute of Biodiversity and Ecology. We are also grateful for the recommendations of the reviewers that have improved our manuscript.

REFERENCES

Almagro M, Maestre FT, Martinez-Lopez J, Valencia E, Rey A (2015) Climate change may reduce litter decomposition while enhancing the contribution of photodegradation in dry perennial Mediterranean grassland. Soil Biol Biochem 90:214–223. https://doi.org/10.1016/j.soilbio.2015.08.006

Austin AT, Vivanco L (2006) Plant litter decomposition in a semi-arid ecosystem controlled by photodegradation. Nature442:555–558. https://doi.org/10.1038/nature05038

Austin AT, Méndez MS, Ballaré CL (2016) Photodegradation alleviates the lignin bottleneck for carbon turnover in terrestrial ecosystems. Proceed Natl Acad Sci USA 113:4392–4397. https://doi.org/10.1073/pnas.1516157113

Baldock JA, Oades JM, Preston CM, Nelson PN, Skene TM, GolchinA, Clark P (1997) Assessing the extent of decomposition of nat-ural organic materials using solid state 13C NMR spectroscopy. Aust J Soil Res 35:1061–1083. https://doi.org/10.1071/S97004

Baldrian P (2006) Fungal laccases-occurrence and properties. FEMS

Microbiol Rev 30:215–242. https://doi.org/10.1111/j.1574-4976.2005.00010.x

Bornman JF, Barnes PW, Robinson SA, Ballaré CL, Flint SD (2014) Solar ultraviolet radiation and ozone depletion-driven climate change: effects on terrestrial ecosystems. Photochem Photobiol Sci 14:88–107. https://doi.org/10.1039/c4pp90034k

Boukhdoud N, Gros R, Darwish T, Farnet Da Silva AM (2016) Effect of agricultural practices and coastal constraints on soil microbial functional properties in Mediterranean olive orchards. Europ J Soil Sci 67:470–477. https://doi.org/10.1111/ejss.12347

Brandt LA, King JY, Milchunas DG (2007) Effects of ultraviolet radiation on litter decomposition depend on precipitation and litter chemistry in a shortgrass steppe ecosystem. Global Change Biol13:2193–2205

Brunel C, Gros R, Ziarelli F, Farnet Da Silva AM (2017) Additive or non-additive effect of mixing oak in pine stands on soil properties depends on the tree species in Mediterranean forests. Sci TotalEnviron 590:676–685CalSol software. Institut National de l' Energie solaire (INES). ines.solaire.free.fr/dataclim_1.php. Accessed May 2021.

Coûteaux MM, Bottner P, Berg B (1995) Litter decomposition, climate and litter quality. Trend in Ecology & Evolution 10:63–66. https://doi.org/10.1016/S0169-5347(00)88978-8

Day TA, Zhang ET, Ruhland CT (2007) Exposure to solar UV-B radiation accelerates mass and lignin loss of Larrea tridentate litter inthe Sonoran desert. Plant Ecol 193:185–194. https://doi.org/10.1007/s11258-006-9257-6

Day TA, Guénon R, Ruhland CT (2015) Photodegradation of plant litter in the Sonoran desert varies by litter type and age. Soil Biol Biochem 89:109–122. https://doi.org/10.1016/j.soilbio.2015.06.029

Day TA, Bliss MS, Tomes AR, Ruhland CT, Guénon R (2018) Desertleaf litter decay: coupling of microbial respiration, water-soluble fractions and photodegradation. Glob Change Biol 24:5454–5470.https://doi.org/10.1111/gcb.14438

Delcourt N, Rébufa C, Dupuy N, Boukhdoud N, Brunel C, AbadieJ, Giffard I, Farnet-Da Silva AM (2019) Infrared spectroscopy as a useful tool to predict land use depending on Mediterranean contrasted

climate conditions: a case study on soils from oliveorchards and forests. Sci Total Environ 686:179–190. https://doi.org/10.1016/j.scitotenv.2019.05.240

Duguay KJ, Klironomos JN (2000) Direct and indirect effects of enhanced UV-B radiation on the decomposing and competitiveabilities of saprobic fungi. Appl Soil Ecol 14:157–164. https://doi.org/10.1016/S0929-1393(00)00049-4

Esch EH, King JY, Cleland EE (2019) Foliar litter chemistry mediates susceptibility to UV degradation in two dominant species from a semi-arid ecosystem. Plant Soil 440:265–276. https://doi.org/10.1007/s11104-019-04069-y

Farnet Da Silva AM, Ferré E, Dupuy N, De La Boussinière A, RébufaC (2017) Infra-red spectroscopy reveals chemical interactions driving water availability for enzyme activities in litters of typical Mediterranean tree species. Soil Biol Biochem 114:72–81. https://doi.org/10.1016/j.soilbio.2017.06.026

Feng X, Hills KM, Simpson AJ, Whalen JK, Simpson MJ (2011) The role of biodegradation and photo-oxidation in the transformation of terrigenous organic matter. Org Geochem 42:262–274. https://doi.org/10.1016/j.orggeochem.2011.01.002

Foereid B, Bellarby J, Meier-Augenstein WKH, Kemp H (2010) Does light exposure make plant litter more degradable? Plant Soil333:275–285. https://doi.org/10.1016/j.soilbio.2011.03.004

Gliksman D, Haenel S, Osem Y, Yakir D, Zangy E, Preisler Y, Grünzweig JM (2017) Litter decomposition in Mediterranean pine forests is enhanced by reduced canopy cover. Plant Soil 422:317–329. https://doi.org/10.1007/s1110.4-017-3366-y

Heredia-Guerrero JA, Guzman-Puyol S, Benítez JJ, Athanassiou A, Heredia A, Domínguez E (2018) Plant cuticle under global change: biophysical implications. Global Change Biol 24:2749–2751

Huang G, Li Y (2017) Photodegradation effects are related to precipitation amount, precipitation frequency and litter traits in desert ecosystem. Soil Biol Biochem 115:383–392. https://doi.org/10.1016/J.SOILBIO.2017.08.034

Huang G, Zhao HM, Li Y (2017) Litter decomposition in hyper-arid deserts: photodegradation is still important. Sci Total Environ601–602:784–792. https://doi.org/10.1016/j.scitotenv.2017.05.213

Hunt JE, Mc Seveny TM (2002) Seasonal changes of UV-absorbing compounds in the leaves of two native trees, UV radiation and its effects: an update 2002. Royal Society of New Zealand, Christchurch, New Zealand, p 124

Jiang H, Pan Y, Liang J, Yang Y, Chen Q, Lv M, Pang L, He W, Tian X (2021) UV radiation doubles microbial degradation of standing litter in a subtropical forest. J Ecol 110:2156–2166. https://doi.org/10.1111/1365-2745.13939

Jolliffe IT (2002) Principal component analysis. Wiley, New York, pp 10–25

Kheir M, Roche P, Ziarelli F, Farnet da Silva AM (2019) Mediterranean coastal conditions and litter type drive litter microbial responses to drought stress. Eur J Soil Sci 12:828

Kheir M, Lerch TZ, Borsali AH, Roche P, Ziarelli F, Zouidi M, FarnetDa Silva AM (2020) Effect of monospecific and mixed litters on bacterial communities' structure and functions under contrasting Mediterranean climate conditions. Appl Soil Ecol 155:103681.https://doi.org/10.1016/j.apsoil.2020.103681

Kirschbaum MUF, Lambie SM, Zhou H (2011) No UV enhancement of litter decomposition observed on dry samples under controlled laboratory conditions. Soil Biol Biochem 43:1300–1307. https://doi.org/10.1016/J.SOILBIO.2011.03.001

Lambie SM, Kirschbaum MUF, Dando J (2014) No photodegradation of litter and humus exposed to UV-B radiation under laboratory conditions: No effect of leaf senescence or drying temperature. Soil Biol Biochem 69:46–53

Lanzalunga O, Bietti M (2000) Photo- and radiation chemical induced degradation of lignin model compounds. J Photochem Photobiol,B 56:85–108. https://doi.org/10.1016/S1011-1344(00)00054-3

Lin Y, King JY, Karlen SD, Ralph J (2015) Using 2D NMR spectros-copy to assess effects of UV radiation on cell wall chemistry during litter decomposition. Biogeochemistry 125:427–436. https://doi.org/10.1007/s10533-015-0132-1

Mao B, Zhao L, Zhao Q, Zeng D (2018) Effects of ultraviolet (UV)radiation and litter layer thickness on litter decomposition of two tree species in a semi-arid site of Northeast China. J Arid Land10:416–428. https://doi.org/10.1007/s40333-018-0054-6

Massiot D, Fayon F, Capron M, King I, Le Calve S, Alonso B, DurandJO, Bujoli BB, Gan Z, Hoatson G (2002) Modelling one- and two-dimensional solid-state NMR spectra. Magn Reson Chem40:70–76

Mathers NJ, Jalota RK, Dalal RC, Boyd SE (2007) 13C-NMR analysis of decomposing litter and fine roots in the semi-arid Mulga Landsof southern Queensland. Soil Biol Biochem 39:993–1006

Pieristè TM, Forey E, Sahraoui ALH, Meglouli H, Laruelle F, DelporteP, Robson TM, Chauvat M (2020a) Spectral composition of sun-light affects the microbial functional structure of beech leaf litter during the initial phase of decomposition. Plant Soil 451:515–530

Pieristè TM, Neimane S, Solanki T, Nybakken L, Jones AG, ForeyE, Chauvat M, Ņečajeva J, Robson TM (2020) Ultraviolet radiation accelerates photodegradation under controlled conditions but slows the decomposition of senescent leaves from forest stands in southern Finland. Plant Physiol Biochem 146:42

Richardson AD, Reeves JB, Gregoire GT (2004) Multivariate analy-es of visible/near infrared (VIS/NIR) absorbance spectra reveal underlying spectral differences among dried, ground conifer needle samples from different growth environments. New Phytol161:291–301. https://doi.org/10.1046/j.1469-8137.2003.00913.x

Sardans J, Grau O, Chen HYH, Janssens IA, Ciais P, Piao S, PenuelasJ (2017) Changes in nutrient concentrations of leaves and roots in response to global change factors. Glob Change Biol 23:3849–3856. https://doi.org/10.1111/gcb.13721

Suseela V, Tharayil N (2018) Decoupling the direct and indirect effects of climate on plant litter decomposition: accounting for stress-induced modifications in plant chemistry. Global Change Biology24:1428–1451. https://doi.org/10.1111/gcb.13923

Wang QW, Pieristè M, Liu C, Kenta T, Robson TM, Kurokawa H(2020) The contribution of photodegradation to litter decomposition in a temperate forest gap and understorey. New Phytolog 229:2625–2636. https://doi.org/10.1111/nph.17022

Wang QW, Robson TM, Pieristè M, Kenta T, Zhou W, Kurokawa H (2022) Canopy structure and phenology modulate the impacts ofs olar radiation on C and N dynamics during litter decomposition in a temperate forest. Sci Total Environ 820:153185. https://doi.org/10.1016/j.scitotenv.2022.153185